Hamsa N. Naser
Rafea T. Ahmed
Jinan A. Abd
Nada A. Mohammed

Department of Laser Physics,
Faculty of Science for Women,
University of Babylon,
Babil, IRAQ

Silver Nanoparticles Effects on Methyl Orange Dye Photocatalysis for Environmental Applications

Silver nanoparticles (AgNPs) were synthesized by one of the most popular technique of pulsed laser ablation in liquids (PLAL) for photodegradation of methyl orange dye. To investigate the surface morphology of the nanoparticles, x-ray diffraction (XRD) and field-emission scanning electron microscopy (FE-SEM) were used. Their results indicated that silver particles have sizes within nanoscale range. While UV spectrophotometer was used to examine the optical characteristics at regular time intervals (30, 60, 90 and 120 min). The UV results of the prepared materials showed that the best absorbance has been obtained for the concertation of 3×10^{-4} mol of dye which has been measured to be ~489nm. Results denoted that the dye degradation efficiency of AgNPs increased as the concentration of Ag increased in the dye solution to be 81% at the ablated time of Ag that equals to 3 mins. This work enhances the reduction of environmental pollution through this technology that can be environmentally friendly.

Keywords: Dye removal; Laser ablation; Silver nanoparticles; Photodegradation
Received: 06 February 2024; **Revised:** 28 March 2024; **Accepted:** 03 April 2024

1. Introduction

In the recent years, rapid development has made nanotechnology research integral to metal nanoparticles. Generally, nanoparticles have a diameter of 1–100 nm with unique properties and they can be described by their massive surface-to-volume ratios in electronic attributes and quantum effects [1]. The distinctive properties of nanoparticles such as high surface area, electrical, magnetic and/or optical properties, high reactivity, morphological and considerable porosity turn them into valuable materials in adsorption, catalysis, sensing and optic-electronic applications [1,2] as well as bring new options in numerous fields: pharmaceutical, agriculture, text, engineering, etc. [3].

Noble-metal nanomaterials with, among others, a bottom-up approach with discrete morphologies such as spheres, cubes, stars and wires; versatility in synthesis; and low cost demonstrate remarkable physical/ chemical properties allowing unique interactions with the ecosystem [4,5]. This is particularly purely made inorganic nanoparticles including gold, silver and copper that have distinctive photothermal and optical characteristics in absorbing a broad area of visible spectrum in the electromagnetic radiation. Gold (Au) and silver (Ag) nanoparticles have magnified the properties of optoelectronic stability and biocompatibility [6]. Silver nanoparticles (AgNPs) hold good antibacterial properties making them useful materials in different fields products for industrial purposes. This includes biomaterials, therapeutics, catalysis, photocatalysis, sensing and dye-sensitized solar cells [7].

Based on that, one of the most successful utilization of (AgNPs) against water/wastewater treatment that pollutants with organic materials and heavy metals. AgNPs works as plasmonic sensors for photocatalysts. This encourages the degradation (oxidation) of dyes and pesticides, amplifying the environmental functions [8,9].

Generally, Methyl orange (MO) is utilized as a coloring agent in many areas. Although, it is a low-toxic agent, it could have toxic effects and slow decomposition upon disintegration when discharged into water bodies leading to some health risks [9,10]. Therefore, Methyl orange (MO) degradation methods need to be investigated. In order to remove colors, adsorption has been used due to different benefits including adaptability and fast action. Accordingly, sorbents showed well- defined, large and also well accepted area. In the current work, silver nanoparticles (AgNPs) have been synthesized by pulsed laser ablation methods (PLAL) in liquids as photodegradation catalysts of Methyl orange (MO) dye and the degradation efficiency of silver nanoparticles (AgNPs) were studied.

2. Experimental Part

To prepare a solution of methyl orange dye with a concentration of 3×10^{-4}, 5×10^{-4} and 7×10^{-4} mol, a 0.00376 g of the dye powder was dissolved in a volume of 10 cm^3 of distilled water according to the relationship:

$$M.W = (M_m \times C \times V)/1000 \quad (1)$$

where M_m is the weight of the dye (g), C is the concentration to be prepared (mol), V is the volume of solvent (cm^3), and M.W is the molecular weight of the dye used (g/mol)

The different concentrations of dye have been obtained using dilution relationship:

$$C_1V_1 = C_2V_2 \quad (2)$$

An immersed pellet of silver has been ablated in 5 ml of distilled water by Nd:YAG laser (1064nm, 80mJ and 5Hz). When the laser pulses strike the silver surface, a plume will be generated with a strong vibration wave that spreads in all directions within the impact area. This plume emits light and noise, forming a visible plume of silver particles that are adsorbed of the surface of the metal and dispersed in all directions within the liquid. It was noted that the color of the solution changes as the nanoparticles concentration increased due to increment of the number of pulses per minutes (for the chosen concetration $3x10^{-4}$ mol, the ablated time was applied for 1, 2, 3 and 4 mins). Figure (1) shows the process of laser ablation of silver nanomaterial and figure (2) displays the samples that used for degradation applications by exposing them to UV source through (30, 60, 90 and 120 min) using $3x10^{-4}$ mol concentration of dye with ablated time 1, 2 and 3 minutes of Ag nanoparticles.

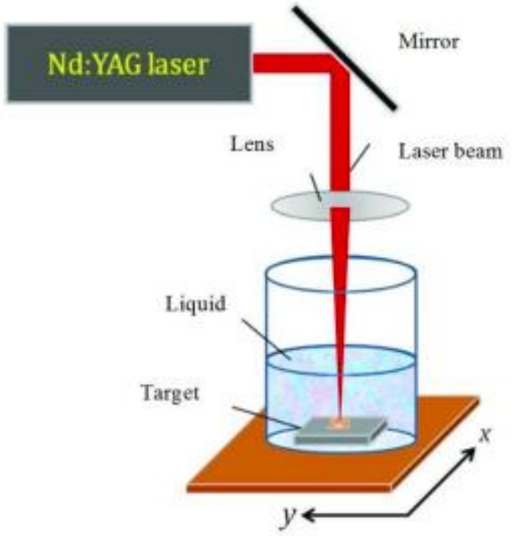

Fig. (1) The pulse laser ablation process

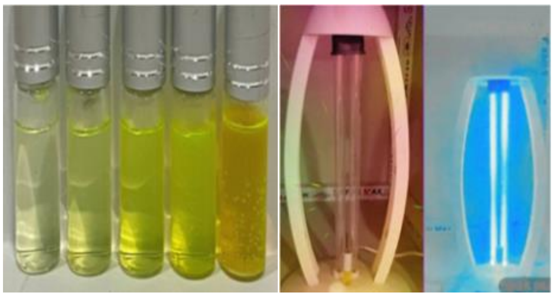

Fig. (2) The samples before and after exposure to UV radiation

3. Results and Discussion

The XRD and FE-SEM tests have been utilized to determine the size of silver particles. Figure (3) presents the XRD pattern, which indicates that the prepared particles are silver nanoparticles and have polycrystalline of face-centered cubic (FCC) structure with notable peaks at 2θ = 37°, 42.5°, 64° and 77° belong to (111), (200), (220) and (311) planes corresponding to (JCPDS File No. 04-0783) [11].

The crystallite size (D) of the silver particles has been calculated using Scherrer's formula, equation (3) [12].

$$D = \frac{0.9\,.\lambda}{\beta\cos\theta} \qquad (3)$$

The calculated crystallite size (D) of preferred orientation along (200) plane indicates that the crystallite size is within the nanoscale and is about (13.24 nm) which is very close to the value of other research [11].

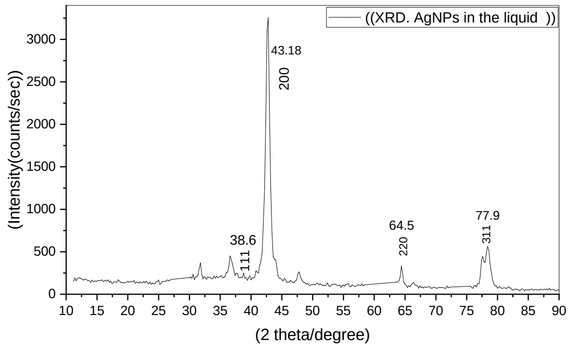

Fig. (3) XRD pattern of silver nanoparticles

FE-SEM images shown in figures (4) and (5) specify that the range of particles sizes smaller than 50 nm according to the device scale. The images show a light emitting and semi-spherical shape of silver nanoparticles. Most metals, including Ag, have FCC structures and grow from nucleation into twinned and multiply twinned particles with surfaces bordered. Ag nanoparticles tend to agglomerate due to the high surface energy and high surface tension of the ultrafine nanoparticles, which may account for the observation of some larger nanoparticles. Catalytic activity, a crucial feature of the produced Ag NPs, is enhanced by their small particle size and wide surface area [13].

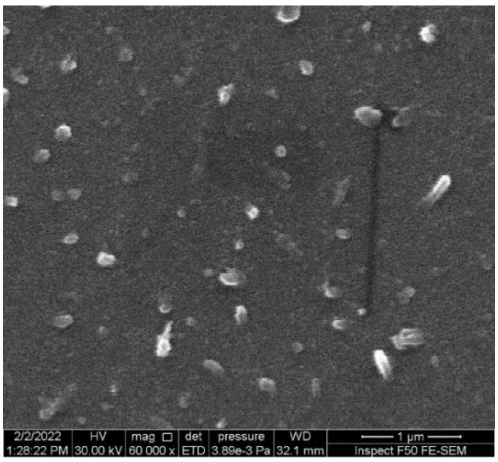

Fig. (4) FE-SEM examination of silver nanoparticles with dimensions of 1µm

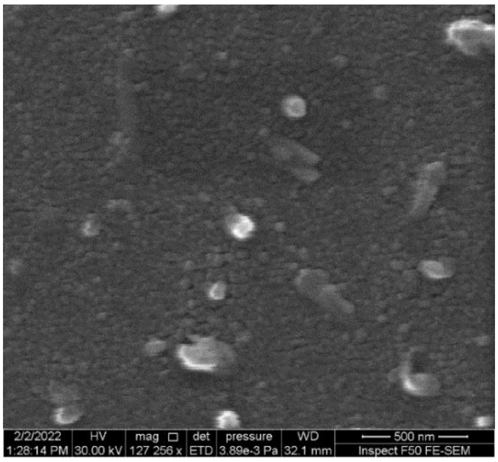

Fig. (5) FE-SEM image of silver nanoparticles with dimensions of 0.5µm

The absorption spectrum as a function of wavelength for methyl orange without and with the prepared Ag nanomaterial were measured using a UV-visible spectrophotometer as shown in figures (6) and (7), respectively. Figure (6) indicates that the absorbance spectrum of dye lies in the range of ~489nm) and figure (7) shows the spectrum of Ag particles lies in the range of ~403nm. The nanomaterial prepared at different times and with constant energy showed that the peak of the absorption spectrum increases with increasing the time-related to the number of pulses directed at the target. This increment contributes to increasing the occurrence of induced defects, and this result is consistent with previous results of other research [13,14].

The transmittance curve for all samples shows an opposite behavior to the absorbance (Fig. 8), as the curve begins to increase at the wavelength of 350 nm and then tends to saturate at wavelengths longer than 550nm, as the transmittance increases with increasing wavelength. These results about transmittance versus wavelength are similar to research [10]. It is also noted that the transmittance decreases with increasing time for the laser pulses directed at the target.

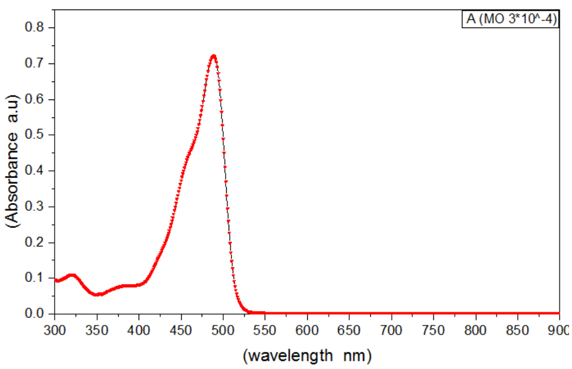

Fig. (6) The absorbance as a function of wavelength of methyl orange dye without Ag nanoparticles

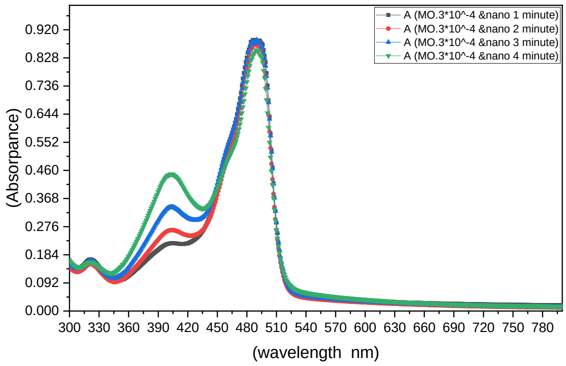

Fig. (7) The absorbance as a function of wavelength of methyl orange dye with Ag nanoparticles

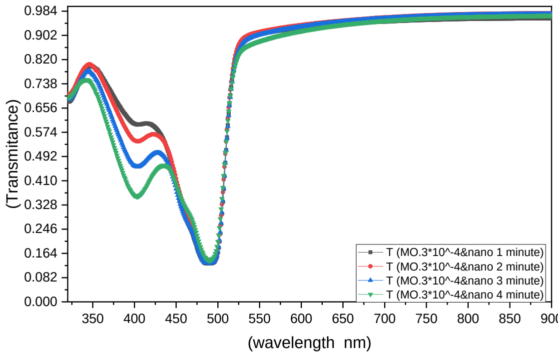

Fig. (8) The transmittance as a function of wavelength of methyl orange dye with Ag nanoparticles

The linear absorption coefficient with wavelength for both the dye and the silver nanoparticles has been calculated using the following equation [1]:

$$\alpha = 2.303\ A/d \qquad (4)$$

The absorption coefficients of all concentrations $\alpha > 10^{6}$ cm^{-1}, as shown in Fig. (9). This result indicates a close relationship between increasing absorption with increasing energy of the incident photon, and this result was noted by other researchers [10,14,15] that this is due to the increased probability of electronic transfer between valence levels to the conduction band with increasing energy of the incident photon. The value of the absorption coefficient is high and increases with increasing ablated time, as can be seen from Fig. (9), and this behavior was monitored by other research [10,16].

The extinction coefficient was found from the relationship [10]:

$$K = \alpha\, \lambda / 4\, \pi \qquad (5)$$

The extinction coefficient changes as a function of the wavelength, as shown in Fig. (10). It is clearly that in the ultraviolet region and at low concentrations, the extinction coefficient has low values and increases with increasing Ag nanoparticles concentration. In the visible region, the extinction coefficient is the highest possible due to the high absorption in this region.

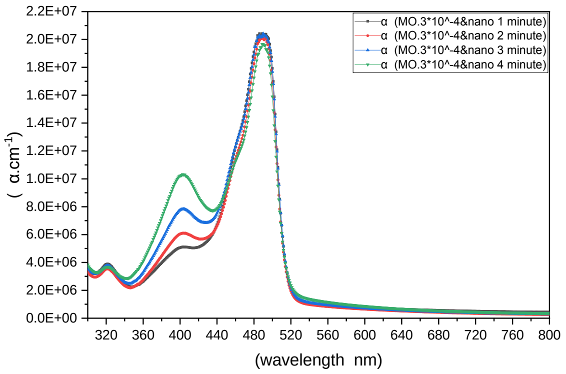

Fig. (9) The absorption coefficient (α) as a function of wavelength of methyl orange dye with Ag nanoparticles

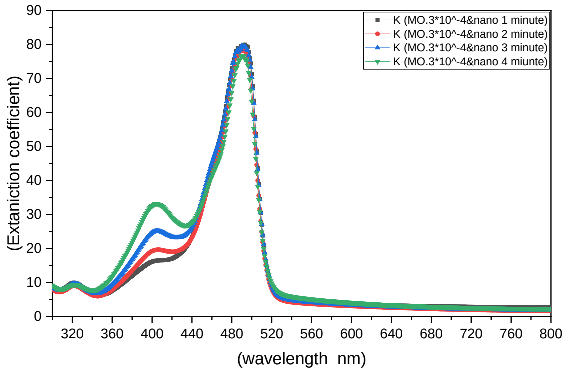

Fig. (10) The extinction coefficient as a function of wavelength of methyl orange dye with Ag nanoparticles

The refractive index has been calculated for the methyl orange dye and Ag nanomaterial. Figure (11) shows the refractive index values as a function of wavelengths within range of 350-500nm. It can be seen that the refractive index increases in the (UV) region. It extends to the visible region, as the concentration of the dye and Ag nanoparticles increase with increasing the time represented by the number of pulses, the value of the refractive index increases as a result of the stacking process that occurs within the crystalline structure. There is also a main reason, which is the increase in reflectivity at the expense of absorbance and optical transmittance.

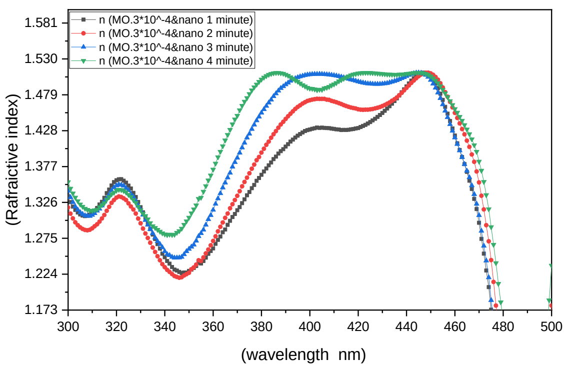

Fig. (11) The refractive index as a function of wavelength of methyl orange dye with Ag nanoparticles

Figure (12) represents the absorption spectrum of methyl orange (MO) dye, where the best concentration of the dye was taken through the absorption spectrum at a concentration of $3x10^{-4}$ mol mixed with different concentrations of Ag nanoparticles for 1, 2 and 3 min ablated time. Figures (12a), (12b) and (12c) represent the absorption spectrum of every concentration of Ag nanoparticles in the MO dye as a catalytic by exposing the samples to UV source through 30, 60, 90 and 120 min. It was observed that the absorption of Ag nanoparticles overlapped with the absorption of the dye at the range of 490 nm, as shown in the figure. The best degradation of dye concentration has been achieved at concentration of Ag nanoparticles of 3 min at 120 min of exposing time due to the adsorption of the dye by the silver nanomaterial which possesses a very high mobility.

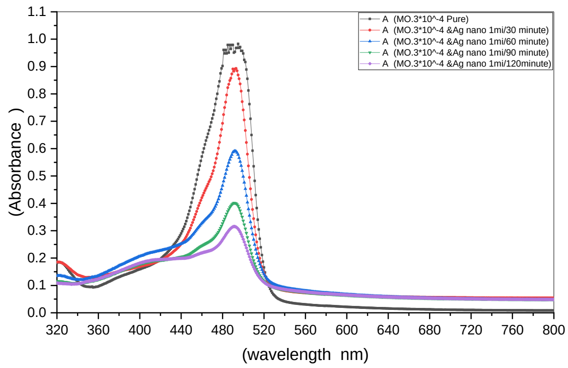

(a) 1 min

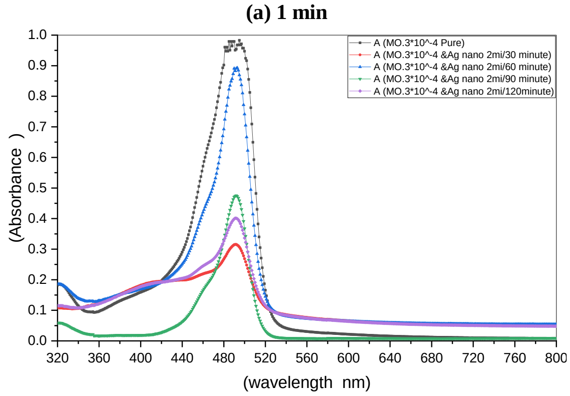

(b) 2 min

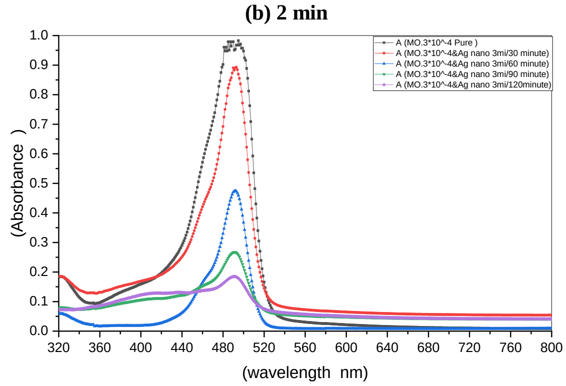

(c) 3min

Fig. (12) The absorbance and wavelength of methyl orange dye and silver nanoparticles after irradiation with UV source for different times

The heat was generated as a result of the absorption of UV light and the response of UV light at different times of Ag nanoparticles due to its plasmonic response, give an indication that Ag nanoparticles are good photocatalyst for degradation applications. This behavior has been observed by Yingying Sha and his group [17] as well as Sini Kuriakose and her group [18].

The ratios of A_t/A_0 for all sample have been tabulated in table (1) and drawn versus irradiation time in Fig. (13). The ratio for all concentrations specify that the photogradation process of dye by Ag nanoparticles increases with increasing of Ag concentration and exposing time to UV light.

Table (1) A_t/A_0 of samples during the irradiation time of ultraviolet source

Intensity of UV	1 minute	2 minute	3 minute
Time (min)	A_t/A_0		
0	1	1	1
30	0.642	0.673	0.793
60	0.543	0.595	0.707
90	0.378	0.452	0.502
120	0.081	0.094	0.133

To calculate the degradation efficiency of Ag nanoparticles (η), the following equation can be used

$$\eta = A_0 - A_t/A_0 \times 100\% \quad (6)$$

A_0 is the absorbance at T= 0, A_t is the absorbance at T=T

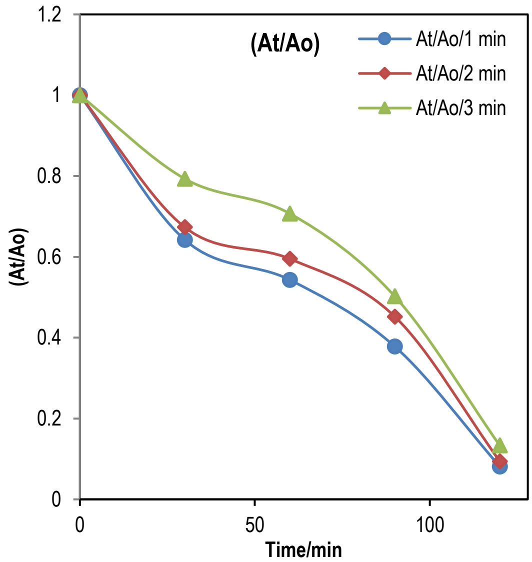

Fig. (13) The ratios of A_t/A_0 of methyl orange dye and silver nanoparticles as a function of irradiation time

Figure (14) is shown the efficiency values for all samples. From this figure, it can be noticed that the efficiency degradation increases up to 81% as the concentration of Ag nanoparticles increasing and the exposing time of every concentration to the UV source increasing.

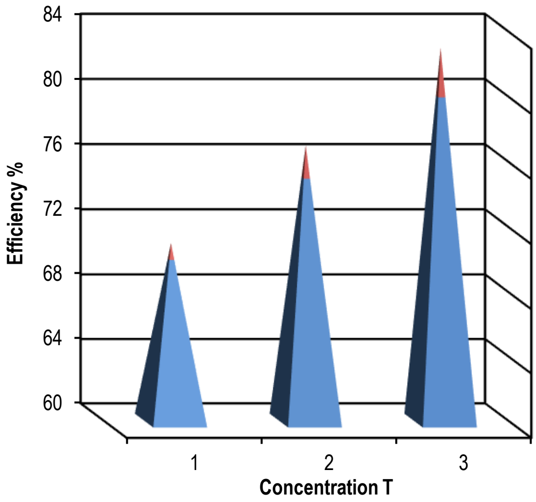

Fig. (14) The degradation efficiency of Ag nanoparticles with different concentrations

4. Conclusions

By studying the effectiveness of the photocatalyst of methyl orange dye and silver nanomaterial, we noticed that the catalytic process was very rapid, as the silver nanomaterial is characterized by strong and rapid absorption of ultraviolet rays for different periods, as the increase in the number of nanoparticles of small dimensions present in its structure, which makes it capable to break down toxic organic pollutants, in addition to the occurrence of the surface plasmon phenomenon, which occurs in noble elements such as silver, and the adsorption process, which has a significant impact on the process of removing organic pollutants and maintaining a clean environment. Nanoparticles of Ag have been successfully synthesized by laser ablation in liquids and used as catalysts. The results obtained show that the methyl orange dye degradation increases as the concentration of the nanoparticles increasing. The results indicate that Ag nanoparticles have the best degradation efficiency of (MO) dye at 120 mins of exposing time to UV source, which is about 81% at 3 mins of ablated time, while the degradation efficiency of 69 % and 75% at 1 and 2 mins of ablated time, respectively.

References

[1] G. Palani et al., “Silver Nanoparticles for Waste Water Management”, *Molecules*, 28 (2023) 3520.
[2] A. Callegari, D. Tonti and M. Chergui, “Photochemically Grown Silver Nanoparticles with Wavelength-Controlled Size and Shape”, *Nano Lett.*, 3 (2003) 1565-1568.
[3] V.K. Sharma and M. Feng, “Water depollution using metal-organic frameworks-catalyzed advanced oxidation processes: A review”, *J. Hazard. Mater.*, 372 (2019) 3-16.
[4] G.M. Nair, T. Sajini and B. Mathew, “Advanced green approaches for metal and metal oxide nanoparticles synthesis and their environmental

applications", *Talanta Open*, 5 (2021) 100080.
[5] L.S. Nair and C.T. Laurencin, "Silver nanoparticles: Synthesis and therapeutic applications", *J. Biomed. Nanotechnol.*, 3 (2007) 301-316.
[6] M. Kedzierska et al., "The Synthesis Methodology of PEGylated Fe_3O_4@Ag Nanoparticles Supported by Their Physicochemical Evaluation", *Molecules,* 26 (2021) 1744.
[7] W. Florkiewicz et al., "Investigation on Green Synthesis, Biocompatibility, and Antibacterial Activity of Silver Nanoparticles Prepared Using Cistus incanus", *Materials*, 14 (2021) 5028.
[8] M. Kedzierska et al., "The Synthesis Methodology and Characterization of Nano gold-Coated Fe_3O_4 Magnetic Nanoparticles", *Materials,* 15 (2022) 3383.
[9] F.H. Hussein, "Photochemical treatments of textile industries wastewater", *Asain J. Chem.*, 24(12) (2012) 5427-5434.
[10] H. Ibrahim, J.A. Abd and A.J.K. Algidsawi, "Fe_2O_3@SiO_2 Nanoparticles: Synthesis and characterization for photodegradation applications", *HIV Nursing*, 23(3) (2023) 1347-1351.
[11] B.K. Mehta et al., "Green synthesis of silver nanoparticles and their characterization by XRD", *J. Phys.: Conf. Ser.,* 836 (2017) 012050.
[12] J.A. Abd and W.M. Mohammed, "Indium oxide: Synthesis and characterization for future industrial applications", *AIP Conf. Proc.*, 2123 (2019) 020010.
[13] N. Nikolay et al., "Laser-assisted fabrication of gold nanoparticle-composed structures embedded in borosilicate glass", *Beilstein J. Nanotech.*, 8 (2017) 2454-2463.
[14] M.M. Al-Mousawi, A. Al-Nafiey and G. Al-Dahesh, "Studying the effect of the number of laser pulses on the structure, morphology, and optical properties for a thin film of GO-Ag nanocomposites", *J. Phys.: Conf. Ser.*, 1 (2021) 1999.
[15] K.M. Reza, A.S.W. Kurny and F. Gulshan, "Parameters affecting the photocatalytic degradation of dyes using TiO_2: A review", *Appl. Water Sci.*, 7 (2017) 1569-1578.
[16] B. Dabirvaziri et al., "A simple and effective synthesis of magnetic γ-Fe_2O_3@SiO_2@TiO_2–Ag microspheres as a recyclable photocatalyst: dye degradation and antibacterial potential", *J. Enviro. Health Sci. Eng.*, 17(2) (2019) 949-960.
[17] Y. Sha et al., "Rapid degradation of azo dye methyl orange using hollow cobalt nanoparticles", *Chemosphere,* 144 (2016) 1530-1535.
[18] S. Kuriakose et al., "Facile synthesis of Ag–ZnO hybrid nano spindles for highly efficient photocatalytic degradation of methyl orange", *Phys. Chem. Chem. Phys.*, 16(33) (2014) 17560 - 17568.